AMERICAN SOCIETY FOR MICROBIOLOGY | Antimicrobial Agents and Chemotherapy®

PHARMACOLOGY

Preclinical Pharmacokinetic and Pharmacodynamic Data To Support Cefoxitin Nebulization for the Treatment of *Mycobacterium abscessus*

Shachi Mehta,[a,b] Vincent Aranzana-Climent,[a,b] Blandine Rammaert,[a,b,d] Nicolas Grégoire,[a,b] Sandrine Marchand,[a,b,c] William Couet,[a,b,c] Julien M. Buyck[a,b]

[a]Inserm U1070, Pôle Biologie Santé, Poitiers, France
[b]UFR Médecine-Pharmacie, Université de Poitiers, Poitiers, France
[c]Service de Toxicologie-Pharmacocinétique, CHU Poitiers, Poitiers, France
[d]Service de Maladies Infectieuses, CHU Poitiers, Poitiers, France

ABSTRACT *Mycobacterium abscessus* is responsible for difficult-to-treat chronic pulmonary infections in humans. Current regimens, including parenteral administrations of cefoxitin (FOX) in combination with amikacin and clarithromycin, raise compliance problems and are frequently associated with high failure and development of resistance. Aerosol delivery of FOX could be an interesting alternative. FOX was administered to healthy rats by intravenous bolus or intratracheal nebulization, and concentrations were determined in plasma and epithelial lining fluid (ELF) by liquid chromatography-tandem mass spectrometry. After intrapulmonary administration, the FOX area under the curve within ELF was 1,147 times higher than that in plasma, indicating that this route of administration offers a biopharmaceutical advantage over intravenous administration. FOX antimicrobial activity was investigated using time-kill curves combined with a pharmacokinetic/pharmacodynamic (PK/PD) type modeling approach in order to account for its *in vitro* instability that precludes precise determination of MIC. Time-kill data were adequately described by a model including *in vitro* degradation, a sensitive (S) and a resistant (R) bacteria subpopulation, logistic growth, and a maximal inhibition-type growth inhibition effect of FOX. Median inhibitory concentrations were estimated at 16.2 and 252 mg/liter for the S and R subpopulations, respectively. These findings suggest that parenteral FOX dosing regimens used in patients for the treatment of *M. abscessus* are not sufficient to reduce the bacterial burden and that FOX nebulization offers a potential advantage that needs to be further investigated.

KEYWORDS *Mycobacterium abscessus*, cefoxitin, nebulization, pharmacokinetics-pharmacodynamics

Mycobacterium abscessus is the most frequent rapidly growing mycobacteria in human pathology (1). This emerging pathogen is mainly responsible for chronic pulmonary infections in patients with cystic fibrosis (1) and is considered a "new antibiotic nightmare" because of its intrinsic resistance to a broad range of antibiotics, including classical antituberculous agents such as ethambutol, pyrazinamide, and isoniazid (2). Presently there is no reliable antibiotic treatment to cure *M. abscessus* pulmonary infections (2–4). In fact, treatment for pulmonary infections caused by *M. abscessus* is not well standardized yet (4, 5). It consists of intravenous (i.v.) administration of amikacin (AMK) and cefoxitin (FOX) in combination with oral administration of clarithromycin (CLR) for several months (4). Unfortunately, this treatment is associated

Citation Mehta S, Aranzana-Climent V, Rammaert B, Grégoire N, Marchand S, Couet W, Buyck JM. 2019. Preclinical pharmacokinetic and pharmacodynamic data to support cefoxitin nebulization for the treatment of *Mycobacterium abscessus*. Antimicrob Agents Chemother 63:e02651-18. https://doi.org/10.1128/AAC.02651-18.

Address correspondence to William Couet, william.couet@univ-poitiers.fr.

Shachi Mehta and Vincent Aranzana-Climent contributed equally to this work.

Received 20 December 2018
Returned for modification 26 March 2019
Accepted 27 April 2019

Accepted manuscript posted online 6 May 2019
Published 24 June 2019

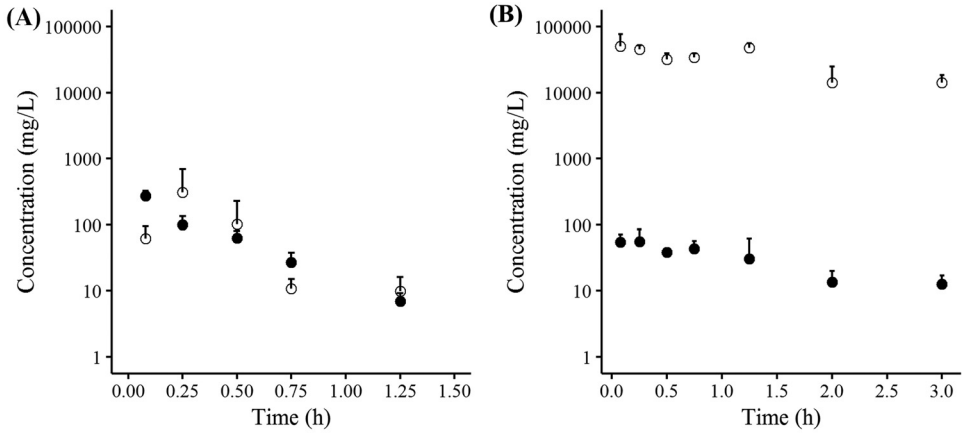

FIG 1 Observed mean concentration ± SD versus time profiles of FOX following i.v. (A) and NEB (B) treatment. Closed symbols correspond to the total plasma concentrations, and open symbols represent ELF concentrations.

with high failure rates, showing infection relapse or death (6). Furthermore, long-term treatments, from several months to a year, with parenterally administered antibiotics are not only challenging and relatively costly but also responsible for low compliance (4). In this context, alternative routes of administration, such as aerosol delivery, should be considered. Nebulization (NEB) is more convenient than i.v. administration and results in higher lung concentrations, and higher efficacy, along with limited systemic side effects, may be achieved (7).

A recent series of well-controlled experiments in healthy rats have shown that antibiotics, such as fluoroquinolones (8), with high membrane permeability are rapidly absorbed after NEB, whereas compounds with much lower membrane permeability, such as colistin (CST) (9), aztreonam (ATM) (10), tobramycin (TOB) (11), gentamicin (GEN), and AMK (12), are slowly absorbed after NEB, leading to high sustained local concentrations, and much higher pulmonary epithelial lining fluid (ELF) concentrations of GEN after NEB than i.v. administration have recently been reported in critically ill patients (13). A simple rule to be considered is that antibiotics that cannot be administered orally, because of poor oral bioavailability due to limited membrane permeability, are, for that same reason, the best candidates for aerosol delivery to treat pulmonary infections. Interestingly, FOX and AMK are rather hydrophilic and are not substantially absorbed after oral administration because of their limited membrane permeability. All of these parameters make FOX as well as AMK good candidates for NEB (12). However, if FOX and AMK present similarities in terms of pharmacokinetics (PK), including low volume of distribution and mostly renal elimination, they do not share similarities in terms of pharmacodynamics (PD). Aminoglycosides, including AMK, are considered to be concentration dependent, whereas β-lactam antibiotics such as FOX are usually supposed to exhibit time-dependent activity (14). Moreover, characterization of FOX activity against *M. abscessus* is made difficult due to its rapid degradation (15, 16) and has been reported only on rare occasions (17–19). Therefore, the objective of this study was first to compare the intrapulmonary PK of FOX after NEB and i.v. administration to healthy rats and then to characterize its *in vitro* PD against a selected strain of *M. abscessus*.

RESULTS

Pharmacokinetics in healthy rats. FOX concentration-time profiles after i.v. administration and NEB are presented in Fig. 1. After i.v. administration, FOX concentrations were almost superimposed in plasma and ELF except at early times due to distribution within ELF. Accordingly, FOX exposure in ELF and plasma was comparable (mean areas under unbound concentration-time curve from time zero to infinity in plasma [$AUC_{u,plasma}$] and ELF [$AUC_{u,ELF}$] of 107 h·μg/ml and 103 h·μg/ml, respectively),

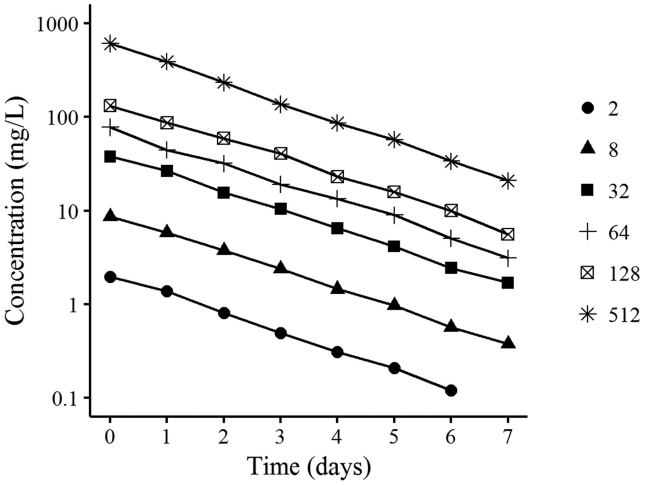

FIG 2 Observed concentration versus time profiles of FOX in 7H9 broth. Initial concentrations of FOX are in mg/liter and indicated by different symbols.

corresponding to a ratio of 1.04. Estimated elimination half-lives in ELF ($t_{1/2}$ = 0.19 h) and plasma ($t_{1/2}$ = 0.23 h) were also virtually identical. After NEB, FOX concentrations were much higher within ELF than in plasma, with $AUC_{u,ELF}$ of 119,289 h·μg/ml and $AUC_{u,plasma}$ of 104 h·μg/ml, corresponding to a ratio of 1,147. Noticeably, $AUC_{u,plasma}$ was identical after NEB and i.v. administration, but the $AUC_{u,ELF}$ was 1,113-fold higher after NEB than after i.v. administration. Again, ELF and plasma concentrations decreased approximately in parallel with time after NEB (Fig. 1), with corresponding half-lives estimated at 1.54 h and 1.23 h, respectively, which is at least 6 times longer than that after i.v. administration.

***In vitro* FOX degradation.** FOX degradation followed first-order kinetics with a half-life estimated at 1.5 days (Fig. 2).

***In vitro* pharmacodynamics. (i) Time-kill kinetics assay.** The first series of time-kill experiments showed no effect for initial FOX concentrations equal to or lower than 16 mg/liter. An initial CFU decay followed by regrowth was observed at day 2 for initial concentrations equal to 32 mg/liter and at day 6 for initial concentrations equal to 64 mg/liter. A decay without regrowth over 8 days was observed for initial concentrations above 128 mg/liter (Fig. 3A). The second series of time-kill kinetics showed that a CFU decay followed by a regrowth occurs for initial FOX concentrations between 12

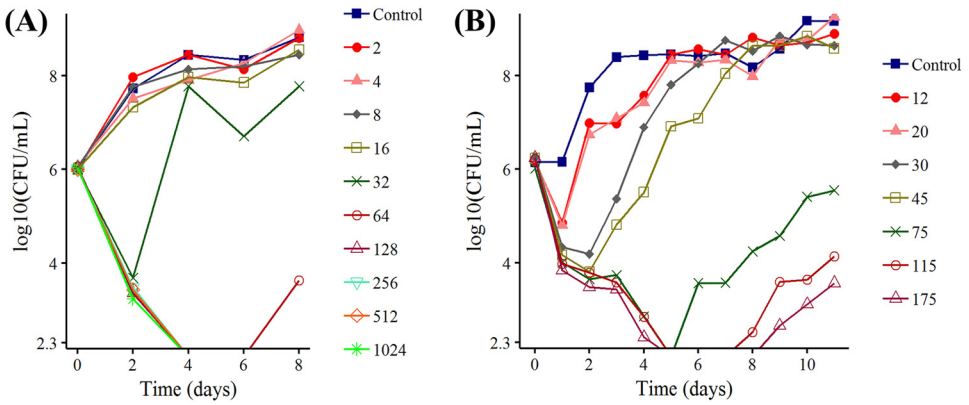

FIG 3 Representative results of FOX time-kill curves against *M. abscessus* CIP 104536 strain. Initial concentrations of FOX are in mg/liter and indicated by different symbols. The ordinate shows the change in the number of CFU (log_{10} scale) per ml of broth. The limit of quantification was 200 CFU/ml (2.3 in log_{10}). (A) First series of experiments. (B) Second series of experiments.

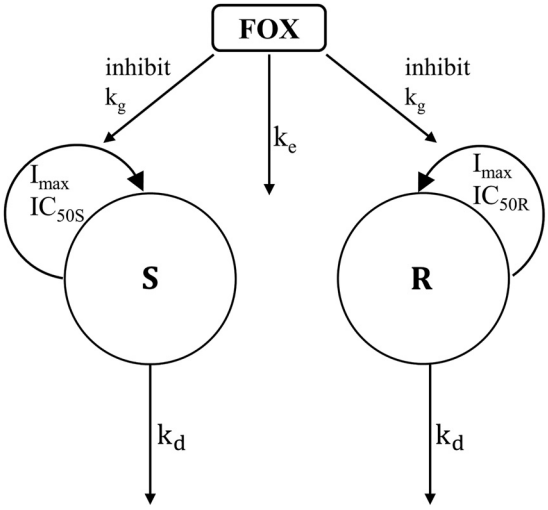

FIG 4 Schematic diagram of the final PK/PD type model. Bacteria multiplied with a first-order rate constant (K_g) in the susceptible (S) and resistant (R) bacterial compartment, and all bacteria had natural death rates (K_d). The cefoxitin compartment (FOX), with a first-order elimination rate (ke), was driving to the bacterial growth inhibition following an I_{max} model.

and 175 mg/liter and that time to regrowth increased with the initial FOX concentrations (Fig. 3B).

(ii) Time-kill modeling. Initially the first series of time-kill kinetics experiments was analyzed using a growth inhibition I_{max} (maximal inhibition) model, with Hill coefficient, with a single homogenous population of bacteria (see the supplemental material). After pooling the two time-kill data sets, a growth inhibition I_{max} model with two subpopulations (Fig. 4), susceptible (S) and resistant (R), best described the experimental data. Visual predictive checks (VPCs) with observed and simulated CFU, with 80% prediction interval, show that model predictions fit the experimental data well, except at a 45-mg/liter initial FOX concentration (Fig. 5). Pharmacodynamics (PD) parameter estimates are presented in Table 1. Noticeably, the difference in susceptibilities of the two bacterial subpopulations is reflected by a 50% inhibitory concentration for the resistant subpopulation (IC_{50R}) 15-fold higher than the IC_{50} for the susceptible subpopulation (IC_{50S}).

(iii) Simulations of CFU versus time profiles without FOX degradation. According to simulations, FOX has no effect on both the S and R subpopulations at a concentration equal to 10 mg/liter and an effect on the S subpopulation only at concentrations equal to 20, 100, or 200 mg/liter (Fig. 6). FOX has no effect on the R subpopulation at concentrations of 20 and 100 mg/liter but has an effect followed by regrowth at a concentration of 200 mg/liter. Complete bacterial killing is expected at 300 mg/liter.

DISCUSSION

The initial PK part of this study has clearly demonstrated a major effect of the route of administration on FOX concentrations within ELF. The targeting advantage (TA) provided by NEB, corresponding to the ratio of $AUC_{u,ELF}$ after NEB versus after i.v. administration and reflecting the relative increased FOX exposure within ELF after NEB, was close to a thousand (TA of 1,113). This high TA is consistent with values previously reported under similar experimental conditions: 242, 2,673, 874, and 162 for TOB (11), ATM (10), AMK, and GEN (12), which are all antibiotics with low membrane permeability precluding oral administration. By comparison, for ciprofloxacin (CIP) and moxifloxacin (MXF), two fluoroquinolone antibiotics with high membrane permeability allowing oral administration, the ratio of $AUC_{u,ELF}$ after NEB versus that after i.v. administration were close to unity (TA of 1.2 for CIP and TA of 0.95 for MXF) (8), suggesting limited, if any,

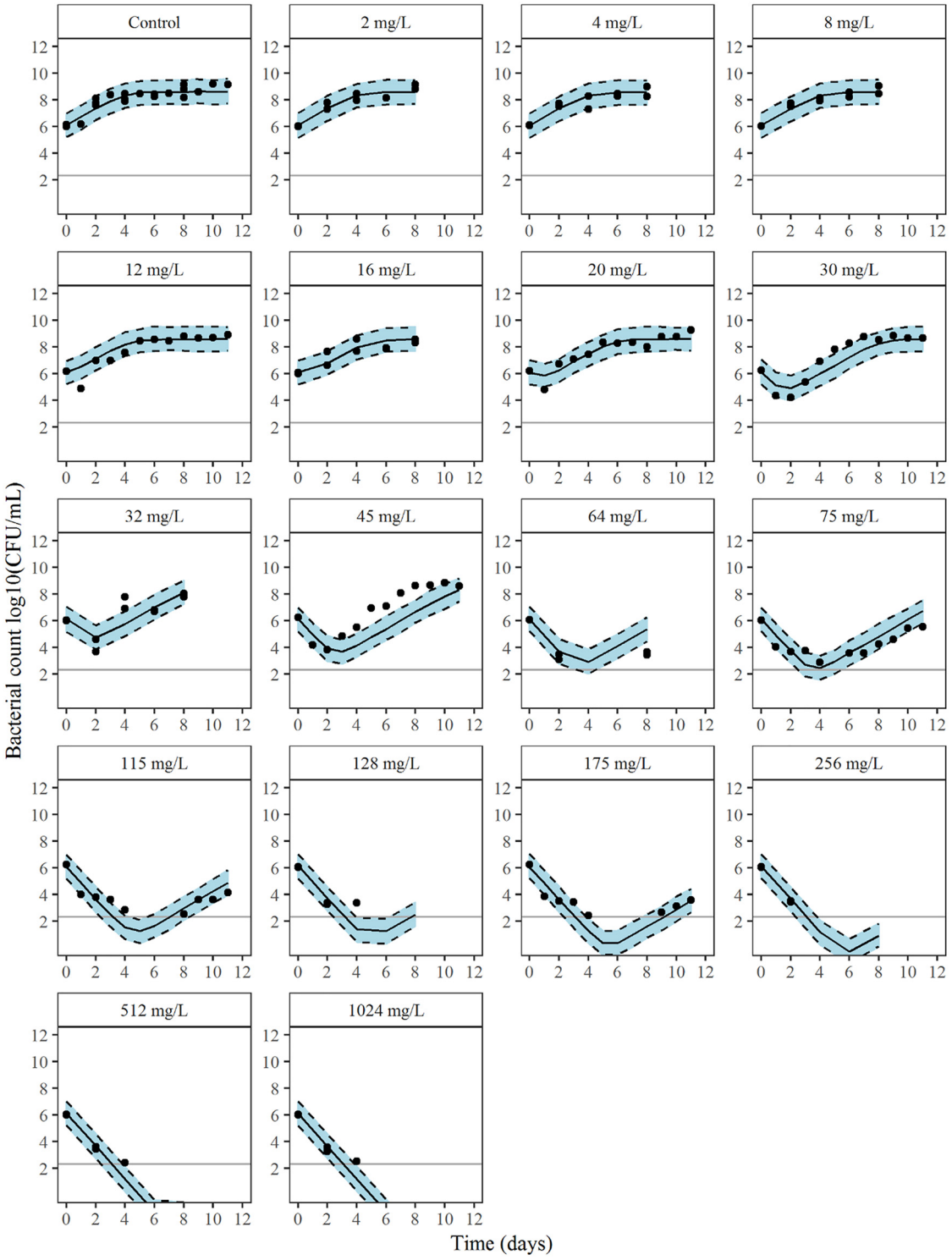

FIG 5 Visual predictive checks (VPCs) for the final PK/PD type model of FOX against *M. abscessus* CIP 104536 with observed bacterial counts (circles), medians (black continuous line), and 80% prediction intervals (black dotted line) of simulated data. Plots include growth control and experimental data by time-kill kinetics. The indicated concentrations are the initial FOX concentrations. The line shows the limit of quantification (200 CFU/ml).

biopharmaceutical advantage of NEB. However, TA values determined in rats after intratracheal administration with the Penn-Century microsprayer cannot be directly extrapolated to humans. Indeed, using this mode of administration, virtually 100% of the dose is absorbed and systemically bioavailable, leading to comparable plasma AUCs

TABLE 1 PD parameter estimations, derived from the growth inhibition model fitted to time-kill kinetics assay

Parameter	Explanation	Estimation (% RSE[a])
LGINOC (log_{10}CFU/ml)	Initial bacterial density	6.1 (1)
K_g (day^{-1})	Bacterial growth rate constant	4.3 (6)
B_{max} (log_{10}CFU/ml)	Bacterial count in stationary phase	9.05 (1)
K_d (day^{-1})	Bacterial death rate constant	2.83 (7)
I_{max}	Maximum fractional reduction of growth by FOX	1 (fixed)
IC_{50S} (mg/liter)	FOX concentration that results in 50% of I_{max} for susceptible subpopulation	16.2 (11)
IC_{50R} (mg/liter)	FOX concentration that results in 50% of I_{max} for resistant subpopulation	252 (20)
K_e (day^{-1})	Degradation rate constant for FOX followed by first-order process	0.438 (fixed)
MUTF	Mutation frequency of bacteria	−9.66 (6)
γ	Hill factor for growth inhibition due to drug activity	4.8 (39)

[a]RSE, relative standard errors.

independent of the route of administration (8–12). This characteristic, which was confirmed in the present study ($AUC_{u,plasma}$ of 103 h·μg/ml after i.v. and 104 h·μg/ml after NEB treatment), does not reflect the clinical setting, with only a small fraction of the dose being absorbed after aerosolization. This can be illustrated by comparing results obtained after nebulization of GEN in rats (12) and patients (13). Comparison of $AUC_{u,plasma}$ values in patients indicates that GEN systemic exposure was close to 5% after NEB compared with i.v. administration.

The PD of FOX, and in particular the potential advantage provided by NEB, not in terms of increased exposure at the infection site but rather in terms of antimicrobial efficacy, was investigated during the second part of this study. Our time-kill results are consistent with those obtained during previous studies over this relatively limited period of time (18, 19). FOX is supposed to be a time-dependent antibiotic, and accordingly it is recommended to maintain concentrations higher than the MIC with no need for high peak concentrations. However, characterization of *in vitro* FOX activity against mycobacterium species is made difficult for two different reasons. Although *M.*

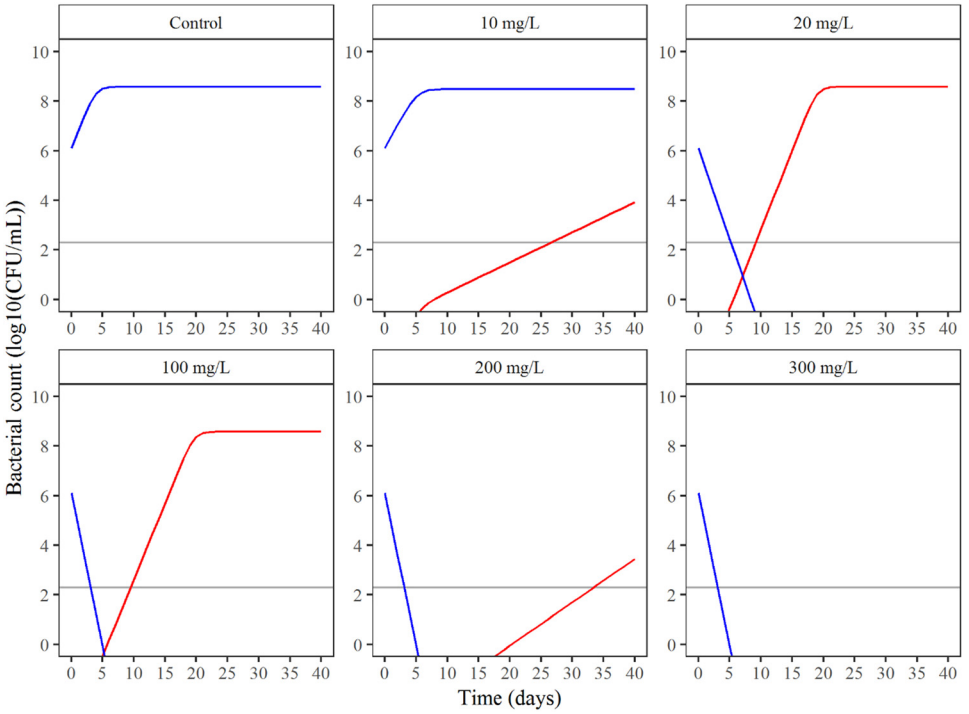

FIG 6 Simulations of CFU counts versus time at several FOX concentrations without considering FOX degradation, using the final PK/PD type model (2 subpopulations) of FOX against *M. abscessus* CIP 104536. Red lines represent the amount of resistant bacteria, and blue lines represent the amount of susceptible bacteria. Horizontal lines show the limit of quantification (200 CFU/ml).

abscessus is considered to be a rapidly growing mycobacterial species, compared with other mycobacteria, such as *M. tuberculosis*, experiments take longer with mycobacterium species than with other bacteria. As an example, MIC determination is conducted over 3 days for *M. abscessus* compared with 1 day for most bacteria. In addition, FOX is degraded within 7H9 broth with an elimination half-life close to 1.5 days, meaning that after 3 days, FOX concentration within the liquid medium would only be 25% of the initial concentration. Actually, FOX degradation within liquid medium was initially documented by Oberholtzer and Brenner (20) and then identified as a real problem for MIC determination by Rominski et al. (15). In fact, when an apparent MIC is reported at 8 mg/liter, it should be noted that this corresponds to the initial FOX concentration, which, after 3 days, or 2 half-lives, should be down to 2 mg/liter. Therefore, the intermediate FOX concentration at 4 mg/liter would better reflect the "true" MIC. In order to take into account this degradation, especially for interpretation of time-kill kinetics experiments conducted over time periods longer than a week, a PK/PD type modeling approach was used. The fact that FOX concentrations decay with time due to *in vitro* first-order degradation was taken into account just as if this was due to *in vivo* elimination. However, the *in vitro* degradation variability was negligible, and the degradation half-life was set at 1.5 days for the PK/PD type modeling, conducted in two separate steps.

Initially, time-kill experiments were conducted at 11 different initial concentrations, from 2 to 1,024 mg/liter, corresponding to multiple values of the apparent MIC, as commonly done (here we used 0.25 to 128 times the MIC), plus a control (Fig. 3). There was virtually no effect at initial concentrations equal to or lower than 16 mg/liter. When the initial concentration was equal to 32 mg/liter, an initial decay of CFU was observed, followed by regrowth after 2 days. For initial concentrations equal to or higher than 64 mg/liter, a CFU decay was observed with no regrowth after 2 days. The question was to determine whether regrowth observed at the intermediate FOX concentration could be explained by its degradation, starting from 32 mg/liter and dropping down to 16 mg/liter and 8 mg/liter after 1.5 and 3 days, respectively. A PK/PD type model was used to answer this question. With this type of model, it can be considered that the antibiotic acts by inhibiting bacterial growth (bacteriostatic effect) or by stimulating bacterial kill (bactericidal effect). Since, according to Lavollay et al. (17) and Greendyke and Byrd (21), FOX is supposed to possess bacteriostatic activity against *M. abscessus*, a growth inhibition PD model was selected with a single homogenous bacterial population. This model provided reasonably good data fitting (see the supplemental material), but noticeably, using the same strain (CIP 104536), Ferro et al. have identified a FOX-resistant subpopulation, preexistent at time zero (22), suggesting that the PK/PD model with a single homogenous bacterial population is not appropriate. However, our initial data set, with regrowth observed at only one FOX concentration, was probably not sufficiently informative to support the superiority of two subpopulations (S and R) versus one population PD model. Therefore, we decided to initiate a second series of time-kill experiments with more intermediate initial FOX concentrations, i.e., susceptible enough to provide initial CFU decay followed by regrowth. Noticeably, according to the one-population model, regrowth should always start at the same FOX concentration (the nadir). Therefore, time to nadir should increase with the initial FOX concentration, more precisely by 1.5 days, corresponding to FOX degradation half-life, each time the initial concentration is increased by twofold. The effect of initial FOX concentration on time to nadir would not be the same in the presence of one and two subpopulations. The supplementary intermediate FOX concentrations used for this second time-kill set of experiments (12, 20, 30, 45, 75, 115, and 175 mg/liter), the frequency of CFU determinations (every day instead of every 2 days), and the experiment duration (increased from 8 to 11 days) were selected in order to allow discrimination between one- and two-population models.

Using the whole data set (initial and second series of time-kill experiments), the two-subpopulation model best described experimental data, as illustrated in Fig. 5.

However, direct interpretation of this figure is difficult, since FOX degradation contributes to regrowth as well as the existence of an R subpopulation. In fact, time-kill experiments are frequently referred to as "static" conditions because they use several different antibiotic concentrations but are stable over time, as opposed to "dynamic" conditions, such as hollow-fiber experiments, in which the medium is replaced in order to let antibiotic concentration decay with time according to 1st-order kinetics, with an elimination half-life selected to mimic *in vivo* PK.

One point of interest in the PK/PD type model was that it allowed simulations of CFU versus time profiles, keeping FOX concentrations constant with time (Fig. 6). It was also possible to simulate the effect of FOX on each subpopulation. Due to the high γ value ($\gamma = 4.8$), the model suggests that a slight change in FOX concentrations around the IC_{50S} (16.2 mg/liter) has dramatic consequences on FOX antimicrobial effect on the S subpopulation. Accordingly, no effect would be expected at a FOX concentration equal to 10 mg/liter, but a marked initial decay of CFU with time with no regrowth is predicted at a FOX concentration equal to 20 mg/liter (Fig. 6). Thus, as far as FOX concentrations remain low compared with the IC_{50R} (252 mg/liter), regrowth of the R subpopulation should be observed at later times (Fig. 6).

Interestingly, after systemic administration at the usual dose (2 g) in patients, FOX total plasma concentrations reach values of up to 200 mg/liter (23), which, considering that the unbound fraction is close to 25% (24), corresponds to maximum unbound plasma concentrations on the order of 50 mg/liter. In this range of values, unbound FOX concentrations should demonstrate antimicrobial efficacy only against the susceptible *M. abscessus* population. Therefore, the possibility of achieving much higher FOX concentrations at the infection site (lung ELF) after nebulization, as suggested in this study using noninfected rats, may offer an opportunity to provide antimicrobial efficacy against the R subpopulation as well.

However, extrapolation of these new data to the clinical setting must be done extremely carefully. First, from a PK standpoint, nebulization with the Penn-Century microsprayer allows good control of the dose, which is of interest for the biopharmaceutical characterization of nebulized antibiotics (8–12, 25) but which does not reflect the clinical setting. Furthermore, on top of potential between-species differences, *M. abscessus* produces biofilm (21), and lung infection induces changes in lung physiology. These phenomena may have an effect on FOX membrane permeability and therefore on lung PK that is not reflected using healthy rats. Second, from a PD point of view, most of our findings rely on a model with a simple two-subpopulation model, which, as previously stated, may be too simplistic. Another limitation of these *in vitro* experiments is that they do not take into consideration the distribution of *M. abscessus* within macrophages or the limited FOX intracellular distribution (19). Finally, in clinical practice *M. abscessus* infections are treated by several antibiotics in combination. This obviously has major consequences in terms of antimicrobial efficacy, which was not addressed here.

In conclusion, the PK/PD type modeling approach developed in this study enabled correction for FOX degradation and, therefore, characterization of the effect-concentration relationship, as is usually done by time-kill experiments. Moreover, combined with the possibility of reaching much higher FOX lung ELF concentrations after nebulization than traditional parenteral administration, it provides evidence to support a potential therapeutic advantage of this route of administration. Furthermore, as far as these high FOX ELF concentrations would not be responsible for undesirable effects, combined with the slow elimination half-life of FOX after NEB, they would allow us to maintain the effect maximum for a long period of time postnebulization. In other words, PK/PD characteristics of FOX may allow spaced nebulization. However, numerous complementary experiments would be necessary to confirm the potential therapeutic advantage of FOX NEB for the treatment of *M. abscessus* infections.

MATERIALS AND METHODS

Antibiotics. FOX sodium salt was obtained from Panpharma (Luitré, France) for *in vivo* and *in vitro* experiments and from Sigma (Saint-Quentin-Fallavier, France) for analytical purposes. Cefuroxime (CXM) was obtained from Aprokam (Clermont-Ferrand, France).

Pharmacokinetics in healthy rats. (i) Administration and sampling. Animal experiments were conducted in compliance with EC Directive 2010/63/EU after approval by the local ethics committee (COMETHEA) and were registered by the French Ministry of Higher Education and Research under authorization number 2015070211159865. Male Sprague Dawley rats ($n = 59$; mean weight of rats, 300 g) from Charles River Laboratories (Saint Germain Nuelles, France) were used for experiments. All rats were divided in two groups corresponding to route of administration (i.v. or NEB) (11). On day 1 of the experiment, FOX sodium salt solutions were prepared in 0.9% NaCl at a concentration of 300 mg/ml for NEB and 30 mg/ml for i.v. administrations. As previously described (9), FOX was administered under isoflurane anesthesia either by i.v. bolus in the tail vein (1 ml) or by intratracheal NEB (100 μl) using a 1A-1B Penn-Century microsprayer (Wyndmoor, USA) at doses commonly used in clinical practices after correction for body weight, close to 90 mg/kg of body weight (23). Bronchoalveolar lavage (BAL) fluid and blood sampling was performed as previously described (8) at various times until 1.25 h after i.v. and 3 h and NEB administration (0.08, 0.25, 0.5, 0.75, and 1.25 h for i.v. and 0.08, 0.25, 0.5, 0.75, 1.25, 2, and 3 h for NEB; 4 to 5 rats were included per time point).

(ii) FOX analytical assay. The FOX analytical assay was conducted by liquid chromatography-tandem mass spectroscopy (LC-MS/MS). The system included a Shimadzu high-performance liquid chromatography (HPLC) module coupled with an API 3500 mass spectrometer (Sciex, Les Ulis, France). An XBridge amide column (3.5 μm; 50- by 2.1-mm inside diameter; Waters, Saint-Quentin en Yvelines, France) was used, and a gradient mobile phase composed of 5 mM ammonium formate and acetonitrile (70:30 [vol/vol]) with 0.01% of formic acid was delivered at 0.4 ml/min. The mass spectrometer was operated in the negative mode. Ions were analyzed by multiple-reaction monitoring (MRM). CXM was used as an internal standard. The transitions were *m/z* 426/156 for FOX and 423/207 for CXM. The standard curve of 0, 0.05, 0.1, 0.5, 1, 5, 15, and 20 mg/liter was performed for BAL fluid and plasma samples. Three levels of concentrations (0.1, 1, and 15 mg/liter) were tested for intraday variability with precision and accuracy of <15% ($n = 18$ per medium). The between-day variability was studied at 0.1, 1, and 15 mg/liter with a precision and bias of <15% ($n = 6$). The urea concentrations in plasma and BAL fluid samples were measured as previously described (9).

(iii) Data analysis. Noncompartmental PK analysis was conducted from time-averaged unbound FOX concentrations. FOX protein binding was fixed at 25% in plasma (24) and considered to be negligible within ELF, in which protein concentration is 10 times lower than that in plasma (26). Mean areas under unbound concentrations versus time from time zero to infinity were estimated using a trapezoidal method with extrapolation to infinity in plasma ($AUC_{u,plasma}$) and ELF ($AUC_{u,ELF}$) using Phoenix WinNonlin 7.0 software (Certara, St. Louis, MO). Elimination rate constants, ke, in plasma and ELF were estimated by least-squares fit of data points (log concentration-time) in the terminal phase of decline. Corresponding apparent elimination half-lives ($t_{1/2}$) were estimated as 0.693/ke. The $AUC_{u,ELF}/AUC_{u,plasma}$ ratios were compared after NEB and i.v. administration, and the TA of NEB compared to that of i.v. was estimated from the ratio of $AUC_{u,ELF}$ after NEB versus i.v. administration (27). Results are presented as means ± standard deviations (SD).

***In vitro* FOX degradation.** For FOX degradation in 7H9 broth, a 10-mg/ml stock solution of FOX sodium salt in water was prepared and stored at −80°C until being thawed for preparing working solutions after appropriate dilutions in 7H9 broth. To evaluate the degradation of FOX in 7H9 broth, individual tubes of 20 ml of 7H9 broth containing 2, 8, 32, 64, 128, and 512 mg/liter of FOX as an initial concentration were inoculated with the bacterial suspension (~1×10^6 CFU/ml) and incubated at 35°C ± 2°C. Samples were collected daily for up to 8 days. FOX concentrations then were measured by the LC-MS/MS analytical method as explained above.

***In vitro* pharmacodynamics. (i) Bacterial strain and suspension preparation.** *M. abscessus* subsp. *abscessus* reference strain CIP 104536 (Collection of Institute Pasteur, Paris, France) was used. Stock vials were conserved at −80°C in Middlebrook 7H9 broth (referred to as 7H9 broth; BD, BBL, Sparks, MD, USA) with 10% oleic acid-bovine albumin-dextrose-catalase (OADC) growth supplement (BD, BBL, Sparks, MD, USA) and 20% glycerol (Carl Roth GmbH Co. KG, Karlsruhe, Germany). *M. abscessus* was grown on Middlebrook 7H11 agar plates (referred to as 7H11 agar plates) with 10% OADC growth supplement and 0.5% glycerol at 30°C for 3 to 5 days. For each experiment, the mycobacterial inoculum was prepared freshly according to CLSI guidelines (28). Briefly, colonies from agar plates were transferred into a hemodialysis tube with 5 to 6 sterile glass beads of 3 nm and then vortexed for 1 min. One ml of sterile water then was added and the mixture incubated for 15 min at room temperature. The bacterial suspension was adjusted to an optical density at 600 nm of 0.10 to 0.15 (~10^8 CFU/ml). Finally, the suspension was diluted to 1/100 to obtain an ~1×10^6 CFU/ml final concentration in appropriate media.

(ii) Time-kill kinetics assay. Individual tubes of 20 ml of 7H9 broth containing 2, 4, 8, 16, 32, 64, 128, 256, 512, and 1,024 mg/liter of FOX as an initial concentration and growth control (CTL) were inoculated with the bacterial suspension (~1×10^6 CFU/ml) and incubated at 35°C ± 2°C under shaking conditions (150 rpm) for up to 8 days. To quantify bacteria at defined time intervals (0, 2, 4, 6, and 8 days), 100-μl samples were taken and diluted serially when appropriate in phosphate-buffered saline (PBS; pH 7.4; Gibco by Life Technologies, France). Samples were then plated on 7H11 agar plates for further CFU counting after 3 to 5 days of incubation at 35°C ± 2°C. The theoretical detection limit was set to 200 CFU/ml, i.e., 2.3 $\log_{10}$ CFU/ml. A second series of experiments was carried out using FOX initial

concentrations of 12, 20, 30, 45, 75, 115, and 175 mg/liter and a growth control using a protocol similar to that explained above. Numbers of CFU were determined daily for up to 11 days.

(iii) Time-kill modeling. CFU counts and FOX concentrations over time were analyzed separately using a nonlinear fixed-effects PK/PD type modeling approach. Parameters were estimated using the first-order conditional estimation (FOCE) method and Laplacian option available in NONMEM version 7.4.1 (Icon Development Solutions Ellicott City, MD, USA). NONMEM project management was made easier using Pirana (29), and CFU counts below the limit of quantification (200 CFU/ml) were handled using Beal's M3 method (30). The degradation of FOX (*C*) during the experiment was modelled as a first-order process:

$$C = C_0 e^{-K_e \times t} \quad (1)$$

Where C_0 is the initial concentration of FOX (mg/liter) spiked in the tube at time zero, K_e is the first-order degradation rate constant (days^{-1}), and t is the corresponding elimination half-life, equal to 0.693/K_e (days). Two bacterial subpopulations were considered: susceptible (S) and resistant (R) bacteria. In the absence of FOX, they were assumed to grow until reaching a plateau, and this was described by a logistic growth function. The effect of FOX on *M. abscessus* CIP 104536 was modelled as an inhibition of bacterial growth, with an I_{max} model and different IC_{50} for each subpopulation. The structure of the PD model is presented in Fig. 5. The differential equations describing variations of susceptible bacterial counts (S) and resistant bacterial counts (R) over time are presented below:

$$\frac{dS}{dt} = K_g \times \left(1 - \frac{B}{10^{B_{max}}}\right) \times \left(1 - \frac{I_{max} \times C^{\gamma}}{IC_{50S}^{\gamma} + C^{\gamma}}\right) \times S - K_d \times S \quad (2)$$

$$\frac{dR}{dt} = K_g \times \left(1 - \frac{B}{10^{B_{max}}}\right) \times \left(1 - \frac{I_{max} \times C^{\gamma}}{IC_{50R}^{\gamma} + C^{\gamma}}\right) \times R - K_d \times R \quad (3)$$

where $B = S + R$ is the total bacterial count (CFU/ml), K_g (day^{-1}) is the bacterial growth rate, K_d (day^{-1}) is the bacterial natural death rate, B_{max} ($\log_{10}$ CFU/ml) is the maximum population size supported by the environment, I_{max} is the maximal inhibition, which was supposed to be total inhibition (I_{max} fixed to 1), and IC_{50S} and IC_{50R} (mg/liter) are the concentrations of FOX for which the effect was 50% of I_{max} for susceptible and resistant bacteria, respectively. The residual variability was described by an additive error model on a $\log_{10}$ scale for bacterial count data and by a proportional error model for concentrations of FOX data. No interexperimental variability was estimated on the parameters because we assumed that it would not be distinguishable from residual variability. Model performance was assessed by the evaluation of the goodness-of-fit plots (e.g., observation versus predictions) and objective function value (OFV). The model was evaluated by performing VPCs with stratification on the type of experiments and FOX concentration. All observations were plotted and overlaid with the median, and 80% prediction intervals were obtained by performing 1,000 simulations of the final model with the original data set as the input.

(iv) Simulations of CFU versus time profiles without FOX degradation. In order to evaluate the effect of FOX on *M. abscessus* at constant concentration, the developed PK/PD type model with two subpopulations was used along with PD parameter estimates to simulate the variation in CFU count over time at different concentrations. R package mrgsolve (31) was used to simulate CFU versus time profiles. The final parameter estimates from the current FOX PK/PD type model with two subpopulations were used to simulate the CFU versus time profiles without considering FOX degradation.

SUPPLEMENTAL MATERIAL

Supplemental material for this article may be found at https://doi.org/10.1128/AAC.02651-18.

SUPPLEMENTAL FILE 1, PDF file, 0.2 MB.

ACKNOWLEDGMENTS

We acknowledge F. Mougari and E. Cambau for their helpful discussion and technical expertise at the initial phase of this project. We thank program Nouvelle Aquitaine CPER 2015-2020 and FEDER 2014-2020 for their participation in LC-MS/MS funding. This work has benefited from the facilities and expertise of the PREBIOS platform (University of Poitiers).

REFERENCES

1. Roux A-L, Catherinot E, Ripoll F, Soismier N, Macheras E, Ravilly S, Bellis G, Vibet M-A, Le Roux E, Lemonnier L, Gutierrez C, Vincent V, Fauroux B, Rottman M, Guillemot D, Gaillard J-L. 2009. Multicenter study of prevalence of nontuberculous mycobacteria in patients with cystic fibrosis in France. J Clin Microbiol 47:4124–4128. https://doi.org/10.1128/JCM.01257-09.
2. Nessar R, Cambau E, Reyrat JM, Murray A, Gicquel B. 2012. Mycobacterium abscessus: a new antibiotic nightmare. J Antimicrob Chemother 67:810–818. https://doi.org/10.1093/jac/dkr578.
3. Jarand J, Levin A, Zhang L, Huitt G, Mitchell JD, Daley CL. 2011. Clinical and microbiologic outcomes in patients receiving treatment for Mycobacterium abscessus pulmonary disease. Clin Infect Dis 52:565–571. https://doi.org/10.1093/cid/ciq237.
4. Griffith DE, Aksamit T, Brown-Elliott BA, Catanzaro A, Daley C, Gordin F, Holland SM, Horsburgh R, Huitt G, Iademarco MF, Iseman M, Olivier K, Ruoss S, von Reyn CF, Wallace RJ, Winthrop K, ATS Mycobacterial Diseases Subcommittee, American Thoracic Society, Infectious Disease Society of America. 2007. An official ATS/IDSA statement: diagnosis, treat-

ment, and prevention of nontuberculous mycobacterial diseases. Am J Respir Crit Care Med 175:367–416. https://doi.org/10.1164/rccm.200604-571ST.
5. van Ingen J, Ferro BE, Hoefsloot W, Boeree MJ, van Soolingen D. 2013. Drug treatment of pulmonary nontuberculous mycobacterial disease in HIV-negative patients: the evidence. Expert Rev Anti Infect Ther 11:1065–1077. https://doi.org/10.1586/14787210.2013.830413.
6. Sfeir M, Walsh M, Rosa R, Aragon L, Liu SY, Cleary T, Worley M, Frederick C, Abbo LM. 2018. Mycobacterium abscessus complex infections: a retrospective cohort study. Open Forum Infect Dis 5:ofy022. https://doi.org/10.1093/ofid/ofy022.
7. Flume PA, VanDevanter DR. 2015. Clinical applications of pulmonary delivery of antibiotics. Adv Drug Deliv Rev 85:1–6. https://doi.org/10.1016/j.addr.2014.10.009.
8. Gontijo AVL, Brillault J, Grégoire N, Lamarche I, Gobin P, Couet W, Marchand S. 2014. Biopharmaceutical characterization of nebulized antimicrobial agents in rats. 1. Ciprofloxacin, moxifloxacin, and grepafloxacin. Antimicrob Agents Chemother 58:3942–3949. https://doi.org/10.1128/AAC.02818-14.
9. Gontijo AVL, Grégoire N, Lamarche I, Gobin P, Couet W, Marchand S. 2014. Biopharmaceutical characterization of nebulized antimicrobial agents in rats. 2. Colistin. Antimicrob Agents Chemother 58:3950–3956. https://doi.org/10.1128/AAC.02819-14.
10. Marchand S, Grégoire N, Brillault J, Lamarche I, Gobin P, Couet W. 2016. Biopharmaceutical characterization of nebulized antimicrobial agents in rats. 4. Aztreonam. Antimicrob Agents Chemother 60:3196–3198. https://doi.org/10.1128/AAC.00165-16.
11. Marchand S, Grégoire N, Brillault J, Lamarche I, Gobin P, Couet W. 2015. Biopharmaceutical characterization of nebulized antimicrobial agents in rats. 3. Tobramycin. Antimicrob Agents Chemother 59:6646–6647. https://doi.org/10.1128/AAC.01647-15.
12. Marchand S, Boisson M, Mehta S, Adier C, Mimoz O, Grégoire N, Couet W. 2018. Biopharmaceutical characterization of nebulized antimicrobial agents in rats. 6. Aminoglycosides. Antimicrob Agents Chemother 62:e01261-18. https://doi.org/10.1128/AAC.01261-18.
13. Boisson M, Mimoz O, Hadzic M, Marchand S, Adier C, Couet W, Grégoire N. 2018. Pharmacokinetics of intravenous and nebulized gentamicin in critically ill patients. J Antimicrob Chemother 73:2830–2837. https://doi.org/10.1093/jac/dky239.
14. Levison ME, Levison JH. 2009. Pharmacokinetics and pharmacodynamics of antibacterial agents. Infect Dis Clin North Am 23:791–797. https://doi.org/10.1016/j.idc.2009.06.008.
15. Rominski A, Schulthess B, Müller DM, Keller PM, Sander P. 2017. Effect of β-lactamase production and β-lactam instability on MIC testing results for Mycobacterium abscessus. J Antimicrob Chemother 72:3070–3078. https://doi.org/10.1093/jac/dkx284.
16. Schoutrop ELM, Brouwer MAE, Jenniskens JCA, Ferro BE, Mouton JW, Aarnoutse RE, van Ingen J. 2018. The stability of antimycobacterial drugs in media used for drug susceptibility testing. Diagn Microbiol Infect Dis 92:305–308. https://doi.org/10.1016/j.diagmicrobio.2018.06.015.
17. Lavollay M, Dubée V, Heym B, Herrmann J-L, Gaillard J-L, Gutmann L, Arthur M, Mainardi J-L. 2014. In vitro activity of cefoxitin and imipenem against Mycobacterium abscessus complex. Clin Microbiol Infect 20:O297–O300. https://doi.org/10.1111/1469-0691.12405.
18. Ferro BE, van Ingen J, Wattenberg M, van Soolingen D, Mouton JW. 2015. Time-kill kinetics of antibiotics active against rapidly growing mycobacteria. J Antimicrob Chemother 70:811–817. https://doi.org/10.1093/jac/dku431.
19. Lefebvre A-L, Dubée V, Cortes M, Dorchêne D, Arthur M, Mainardi J-L. 2016. Bactericidal and intracellular activity of β-lactams against Mycobacterium abscessus. J Antimicrob Chemother 71:1556–1563. https://doi.org/10.1093/jac/dkw022.
20. Oberholtzer ER, Brenner GS. 1979. Cefoxitin sodium: solution and solid-state chemical stability studies. J Pharm Sci 68:863–866. https://doi.org/10.1002/jps.2600680720.
21. Greendyke R, Byrd TF. 2008. Differential antibiotic susceptibility of Mycobacterium abscessus variants in biofilms and macrophages compared to that of planktonic bacteria. Antimicrob Agents Chemother 52:2019–2026. https://doi.org/10.1128/AAC.00986-07.
22. Ferro BE, Srivastava S, Deshpande D, Pasipanodya JG, van Soolingen D, Mouton JW, van Ingen J, Gumbo T. 2016. Failure of the amikacin, cefoxitin, and clarithromycin combination regimen for treating pulmonary Mycobacterium abscessus infection. Antimicrob Agents Chemother 60:6374–6376. https://doi.org/10.1128/AAC.00990-16.
23. Brunetti L, Kagan L, Forrester G, Aleksunes LM, Lin H, Buyske S, Nahass RG. 2016. Cefoxitin plasma and subcutaneous adipose tissue concentration in patients undergoing sleeve gastrectomy. Clin Ther 38:204–210. https://doi.org/10.1016/j.clinthera.2015.11.009.
24. Schrogie JJ, Rogers JD, Yeh KC, Davies RO, Holmes GI, Skeggs H, Martin CM. 1979. Pharmacokinetics and comparative pharmacology of cefoxitin and cephalosporins. Rev Infect Dis 1:90–98. https://doi.org/10.1093/clinids/1.1.90.
25. Galindo Bedor DC, Marchand S, Lamarche I, Laroche J, Pereira de Santana D, Couet W. 2016. Biopharmaceutical characterization of nebulized antimicrobial agents in rats. 5. Oseltamivir carboxylate. Antimicrob Agents Chemother 60:5085–5087. https://doi.org/10.1128/AAC.00909-16.
26. Zhang R, Ghosh SN, Zhu D, North PE, Fish BL, Morrow NV, Lowry T, Nanchal R, Jacobs ER, Moulder JE, Medhora M. 2008. Structural and functional alterations in the rat lung following whole thoracic irradiation with moderate doses: injury and recovery. Int J Radiat Biol 84:487–497. https://doi.org/10.1080/09553000802078396.
27. Yapa S, Li J, Patel K, Wilson JW, Dooley MJ, George J, Clark D, Poole S, Williams E, Porter CJH, Nation RL, McIntosh MP. 2014. Pulmonary and systemic pharmacokinetics of inhaled and intravenous colistin methanesulfonate in cystic fibrosis patients: targeting advantage of inhalational administration. Antimicrob Agents Chemother 58:2570–2579. https://doi.org/10.1128/AAC.01705-13.
28. National Committee for Clinical Laboratory Standards. 2003. Susceptibility testing of mycobacteria, nocardiae, and other aerobic actinomycetes; approved standard. NCCLS document M24-A. National Committee for Clinical Laboratory Standards, Wayne, PA.
29. Keizer RJ, van Benten M, Beijnen JH, Schellens JHM, Huitema A. 2011. Piraña and PCluster: a modeling environment and cluster infrastructure for NONMEM. Comput Methods Programs Biomed 101:72–79. https://doi.org/10.1016/j.cmpb.2010.04.018.
30. Beal SL. 2001. Ways to fit a PK model with some data below the quantification limit. J Pharmacokinet Pharmacodyn 28:481–504. https://doi.org/10.1023/A:1012299115260.
31. Baron KT. 2019. mrgsolve: simulate from ODE-based population PK/PD and systems pharmacology models. https://mrgsolve.github.io/.